Nucleic Acids Research, 1993, Vol. 21, No. 3 601–606

Effect of a 5′-phosphate on the stability of triple helix

Kyonggeun Yoon*, Cheryl A.Hobbs, Amy E.Walter[1] and Douglas H.Turner[1]
Department of Molecular Biology, Sterling Winthrop Pharmaceuticals Research Division, 9 Great Valley Parkway, Malvern, PA 19355 and [1]Department of Chemistry, University of Rochester, Rochester, NY 14627, USA

Received October 7, 1992; Revised and Accepted December 18, 1992

ABSTRACT

An effect of 5′-phosphorylation on the stability of triple helical DNA containing pyrimidine:purine:pyrimidine strands has been demonstrated by both gel electrophoresis and UV melting. A 5′-phosphate on the purine-rich middle strand of a triple helix lowers the stability of triple helix formation by approximately 1 kcal/mol at 25°C. The middle strand is involved in both Watson-Crick and Hoogsteen base pairing. In contrast, a 5′-phosphate on the pyrimidine-rich strands, which are involved in either Watson-Crick or Hoogsteen base pairing, has a smaller effect on the stability of triple helix. The order of stability is: no phosphate on either strand > phosphate on both pyrimidine strands > phosphate on purine strand > phosphate on all three strands. Differential stability of triple helix species is postulated to stem from an increase in rigidity due to steric hindrance from the 5′-phosphate. This result indicates that labelling with ^{32}P affect equilibrium in triplex formation.

INTRODUCTION

Homopurine and homopyrimidine sequences of DNA or RNA have been shown to adopt a triple helix structure, in which a third strand of DNA or RNA base pairs with a double-helix using a Hoogsteen base-pairing scheme (1–4). Pyrimidine oligonucleotides bind in the major groove of Watson-Crick double-stranded DNA. Specificity arises from Hoogsteen hydrogen bonding (3), in which thymine in the third strand recognizes adenine-thymine base pairs in double-stranded DNA (T:AT triplet) and protonated cytosine in the third strand recognizes guanine-cytosine base pairs (C^+:GC triplet) (1–7). It has also been shown that purine oligonucleotides in the third strand can also bind to purines in duplex DNA (A:AT and G:GC triplets) (8–12). Thus far, approaches at gene regulation via triple helix formation have been primarily limited to tracts of homopurine or homopyrimidine sequences.

Recently, we described a gel electrophoresis method for determining the recognition pattern for third strand bases in a triple helix motif (13). The method relies upon detection of single, double and triple strands by their differential mobilities in the gel matrix. In principle, several methods can be used for detection. Surprisingly however, we found that the results depended on whether detection was by silver staining or autoradiography. Here we report that the reason for this anomaly is that the stability of triple helix is dependent upon the 5′-phosphorylation of the strands of triplex comprising a pyrimidine:purine:pyrimidine configuration. In particular, 5′-phosphorylation of the purine strand lowers triplex stability more than phosphorylation of the pyrimidine strands.

MATERIALS AND METHODS

Oligodeoxynucleotides

Oligodeoxynucleotides were purchased from Midland Certified Reagent Company. The reported extinction coefficent for poly(dA) [$\epsilon_{257}=8600$ cm^{-1} (mole base/l)$^{-1}$] was used in the determination of concentration of unphosphorylated and phosphorylated $A_{10}TA_{10}$ and $A_{10}CA_{10}$ (14). The extinction coefficient for poly(dT) [$\epsilon_{265}=8700$ cm^{-1} (mole base/l)$^{-1}$] was used for unphosphorylated and phosphorylated $T_{10}AT_{10}$ and $T_{10}GT_{10}$ (15). Oligonucleotides were end-labelled wth ^{32}P-ATP using T4 polynucleotide kinase.

Electrophoretic analysis of triplex formation

Various amounts of oligonucleotides were combined in a total volume of 10 μl in annealing buffer containing 0.15 M NaCl, 10 mM $MgCl_2$, and 5 mM Tris-acetate pH 7.0. In each pair, a trace amount (~20 ng) of ^{32}P-labelled oligonucleotide, either A or T strand, was included in addition to equal amounts of unlabelled oligonucleotide. The oligonucleotide mixtures were heated at 70°C for 15 min, slow cooled to room temperature, and incubated at 4°C overnight. Annealing was followed by addition of 2 μl of the annealing buffer containing 30% glycerol and 0.25% bromophenol blue. 5 μl of each oligonucleotide mixture was analyzed by gel electrophoresis at 4°C using prechilled 12% polyacrylamide gels (19:1 ratio of acrylamide to bis-acrylamide; 20×20×0.15 cm). Electrophoresis was performed in a buffer containing 50 mM Tris, 50 mM boric acid, and 5 mM $MgCl_2$, pH 8.3 at a constant voltage of 10 V/cm with

* To whom correspondence should be addressed at: Department of Molecular and Cell Biology, Apollon, Inc., 200 Great Valley Parkway, Malvern, PA 19355, USA

a current of 20 to 30 mA. Following electrophoresis, gels were stained using a Bio-Rad silver staining kit according to manufacturer's specifications.

Optical melting curves

Absorbance vs. temperature curves were measured at 259 nm with a heating rate of 1°C per minute in a Gilford 250 spectrophotometer interfaced with a Gilford 2527 thermoprogrammer. Oligonucleotides were dissolved in the same annealing buffer solution used for the gel electrophoresis analysis, 0.15 M NaCl, 10 mM $MgCl_2$, and 5 mM Tris-acetate pH 7.0. Thermodynamic parameters were obtained from melting curves by fitting to a two-state model with linear sloping base lines (16). Most sequences were studied at a single concentration. For triplex formation comprised of single stranded DNA and the duplex targets, $A_{10}CA_{10}$:$T_{10}GT_{10}$ and $pA_{10}CA_{10}$:$T_{10}GT_{10}$, the values for thermodynamic parameters were obtained by averaging the enthalpy and entropy changes obtained from fits of melting curves at several concentrations and from plots of the concentration dependence of the melting temperature (17): $1/T_m = (2.3R/\Delta H°) \log [(2/3) (C_t/4)] + \Delta S°/\Delta H°$, where C_t is the total strand concentration and T_m is the temperature at which half of the original triplex has dissociated to duplex and single strand. The factor of (2/3) in the log term arises because the equilibrium involves association of a duplex and a single strand to form triplex and the total concentration of T strands is twice the concentration of A strand.

RESULTS

In order to establish the stoichiometry of triplex DNA, mixtures of different molar ratios of deoxyoligonucleotides, A and T strands of 21 nucleotides in length ($A_{10}XA_{10}$ and $T_{10}YT_{10}$, where XY = AT, GC, CG, TA), were incubated at 4°C, separated by gel electrophoresis according to mobility, and visualized by silver staining and autoradiography as described in Materials and Methods. The mixture containing an equimolar ratio of $A_{10}TA_{10}$ and $T_{10}AT_{10}$ was detected as a duplex, whereas the mixtures containing a molar excess of $T_{10}AT_{10}$ with respect to $A_{10}TA_{10}$ resulted in the conversion of duplex to a complex of slower mobility detected by silver-staining, as shown in Fig. 1a. The mobility of this complex was invariant among mixtures containing a molar excess of $T_{10}AT_{10}$, indicating a constant stoichiometry of 2:1:

$$\begin{array}{ccc} T_{10} & Y & T_{10} \\ A_{10} & X & A_{10} \\ T_{10} & Y & T_{10} \end{array}$$

Thus, a complex containing a mismatch in the middle position (Y:XY = A:TA) produced a species which migrated as a higher molecular weight complex as compared to duplex, indicating the T_{10}:$A_{10}T_{10}$ interaction on both sides of the mismatch is sufficient to stabilize triplex formation at 4°C.

In addition to an equal amount of unlabelled oligonucleotides, the reaction mixtures in each pair contained a trace amount of ^{32}P-labelled oligonucleotide: the 5′-end-labelled A or T strand was added to the reaction mixtures corresponding to the odd and even numbered lanes, respectively (Fig. 1). Thus, detection of species was carried out by both silver staining and autoradiography of the same gel. Surprisingly, silver staining and autoradiography exhibited differences in the detection of the triplex as demonstrated by comparing lanes 5–10 of Figs. 1a and 1b. Silver staining detected the same amount of triple helix

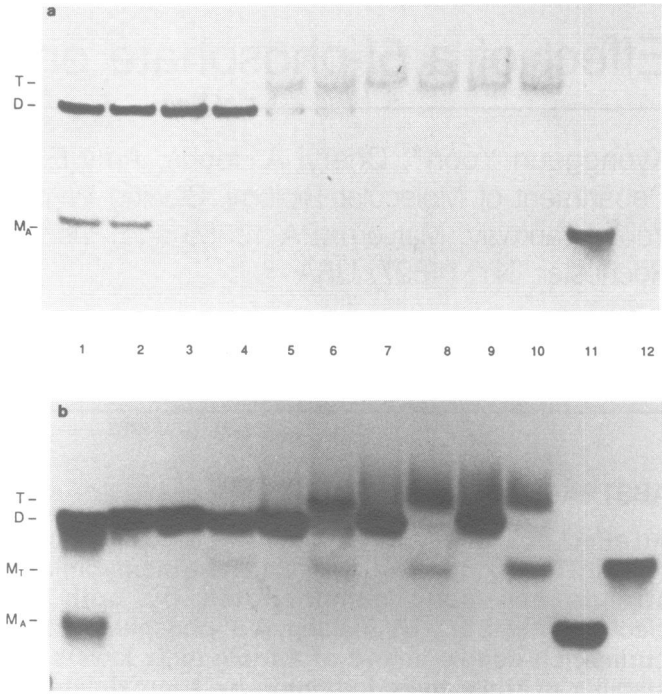

Figure 1 a. Silver stained 12% polyacrylamide gel showing complexes of differing mobility formed by combining 1 μg of $A_{10}TA_{10}$ with increasing amounts of $T_{10}AT_{10}$. The ratios of $A_{10}TA_{10}$ to $T_{10}AT_{10}$ are: 1:0.5 (lanes 1, 2); 1:1 (lanes 3, 4); 1:1.5 (lanes 5, 6); 1:2 (lanes 7, 8); and 1:3 (lanes 9, 10). For each pair, odd and even lanes contain a trace amount of ^{32}P-labelled A or T strand, respectively. Single-stranded $A_{10}TA_{10}$ and $T_{10}AT_{10}$ are shown in lanes 11 and 12, respectively. The species are labelled according to their mobilities: T (triplex), D (duplex), M_A (single-stranded $A_{10}TA_{10}$), or M_T (single-stranded $T_{10}AT_{10}$). Single-stranded $T_{10}AT_{10}$ was not detectable by silver staining but was detected by autoradiography. The formation of complex and gel electrophoresis were carried out as described in Materials and Methods. **b.** Autoradiogram of the identical gel shown in Fig. 1a.

for each pair (Fig. 1a: lanes 5, 6; lanes 7, 8; and lanes 9, 10). In contrast, autoradiography revealed a clear difference in the amount of triple helix formation for each pair (Fig. 1b: lanes 5, 6; lanes 7, 8; and lanes 9, 10). These differences were due to the trace amount of ^{32}P-labelled oligonucleotides included in the reaction mixtures: the triple helix was detected by ^{32}P-labelled $T_{10}AT_{10}$ but not by ^{32}P-labelled $A_{10}TA_{10}$. Thus, a triple helix composed of phosphorylated T strands appears to be more stable than the same triple helix containing a phosphorylated A strand.

Mixtures containing molar ratios in which $A_{10}TA_{10}$ was in excess of $T_{10}AT_{10}$ did not result in the formation of a higher molecular weight complex, as shown in Fig. 2. Under the conditions of this experiment, only a triple helix containing two T strands and one A strand was detected by silver staining (Fig 2a: lanes 1 and 2). Once again, however, the triple helix species containing a mismatch (A:TA triplet) in the middle of the sequence was detected differentially by autoradiography, dependent upon the 5′-phosphorylation of either the A or the T strand (Fig. 2a: lanes 1, 2; Fig. 2b: lanes 1, 2).

Differential stability of triple helix species resulting from the 5′-phosphorylation of either the A or the T strand was demonstrated for other triplet combinations as well. The titration of the two strands, $A_{10}CA_{10}$ and $T_{10}GT_{10}$, shown in Figs. 3 and 4, exhibited triple helix species, regardless of the G:CG mismatch, indicating that the T_{10}:$A_{10}T_{10}$ interaction flanking the

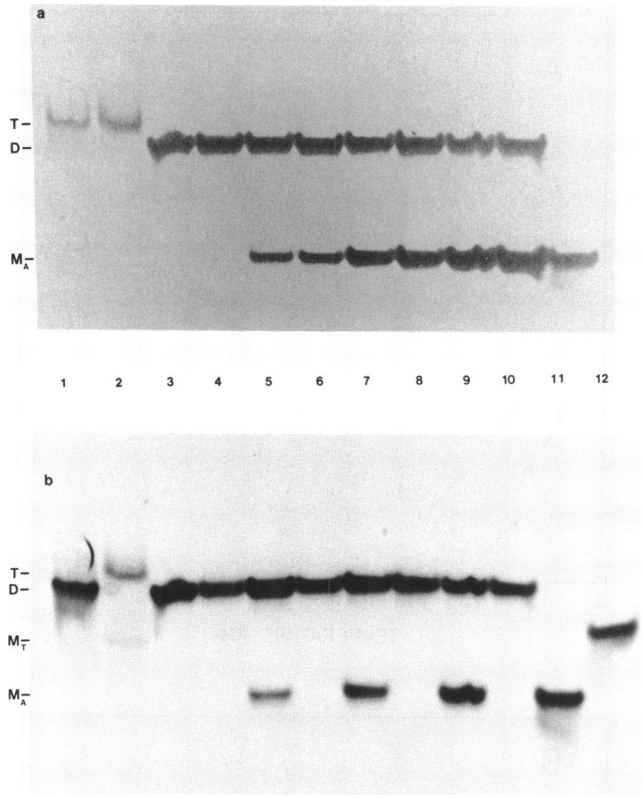

Figure 2 a. Silver stained 12% polyacrylamide gel showing complexes of differing mobility formed by combining 1 μg of $T_{10}AT_{10}$ with increasing amounts of $A_{10}TA_{10}$. The ratios of $T_{10}AT_{10}$ to $A_{10}TA_{10}$ are: 1:0.5 (lanes 1, 2); 1:1 (lanes 3, 4); 1:1.5 (lanes 5, 6); 1:2 (lanes 7, 8); and 1:3 (lanes 9, 10). For each pair, odd and even lanes contain a trace amount of ^{32}P-labelled A or T strand, respectively. Single-stranded $A_{10}TA_{10}$ and $T_{10}AT_{10}$ are shown in lanes 11 and 12, respectively. **b.** Autoradiogram of the identical gel shown in Fig. 2a.

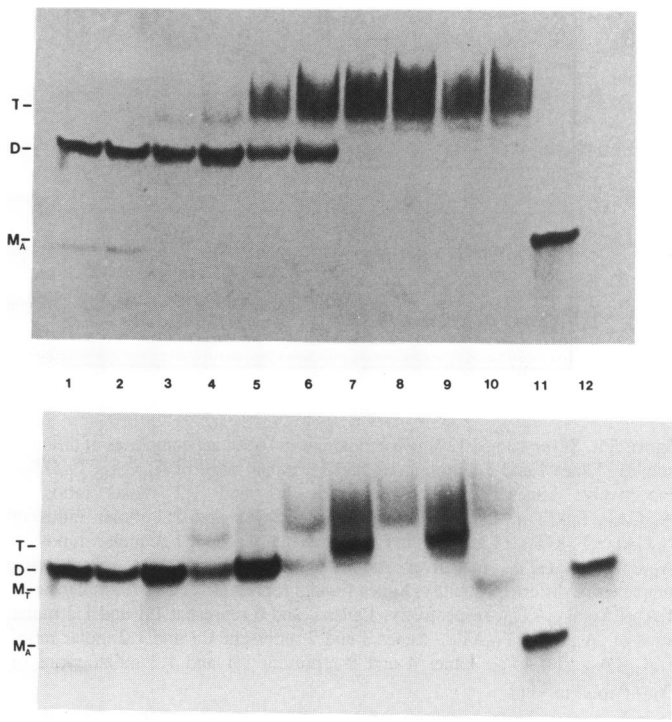

Figure 3 a. Silver stained 12% polyacrylamide gel showing complexes of differing mobility formed by combining 1 μg of $A_{10}CA_{10}$ with increasing amounts of $T_{10}GT_{10}$. The ratios of $A_{10}CA_{10}$ to $T_{10}GT_{10}$ are: 1:0.5 (lanes 1, 2); 1:1 (lanes 3, 4); 1:1.5 (lanes 5, 6); 1:2 (lanes 7, 8); and 1:3 (lanes 9, 10). For each pair, odd and even lanes contain a trace amount of ^{32}P-labelled A or T strand, respectively. Single-stranded $A_{10}CA_{10}$ and $T_{10}GT_{10}$ are shown in lanes 11 and 12, respectively. **b.** Autoradiogram of the identical gel shown in Fig. 3a.

mismatch is sufficient to stabilize triplex formation at 4°C. As before, a triple helix containing two T strands and one A strand was detected. Comparison of silver staining and autoradiography of the same gel demonstrates differential detection of the triple helix for each pair, illustrated in Figs. 3a and 3b (lanes 3, 4; lanes 5, 6; lanes 7, 8; and lanes 9, 10) and Figs. 4a and 4b (lanes 1, 2 and lanes 3, 4). Furthermore, these differences resulted from the trace amount of ^{32}P-labelled oligonucleotides, in a similar manner to that observed for the triplex species containing an A:TA mismatch described above: the triple helix was detected by ^{32}P-labelled $T_{10}GT_{10}$ but not by ^{32}P-labelled $A_{10}CA_{10}$. We also observed differential stability of triple helix species containing canonical triplets (Y:XY=T:AT and C:GC) resulting from the 5′-phosphorylation of either the A or the T strand (data not shown). However, the differential effect on triplex stability observed for stable canonical triplets was not as pronounced as that observed for triplex involving mismatch triplets (Y:XY=A:TA and G:CG).

To this point, the dependence of triple helix stability on the 5′-phosphorylation of either the A or the T strand was demonstrated by using a trace amount of ^{32}P-labelled deoxyoligonucleotides in combination with a comparatively large amount of unlabelled deoxyoligonucleotides. In order to eliminate any possible effects due to the low concentrations of ^{32}P-labelled deoxyoligonucleotides, we performed an experiment using fully phosphorylated A and/or T strands. This time, dependence of

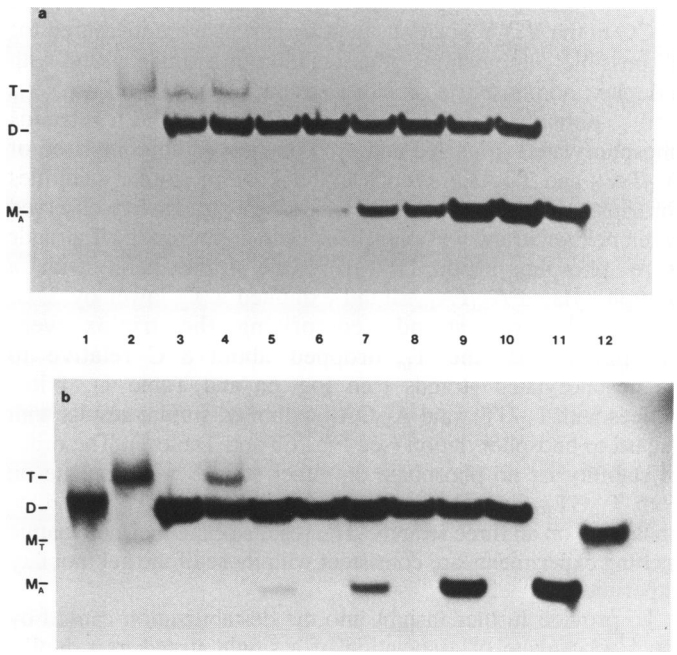

Figure 4 a. Silver stained 12% polyacrylamide gel showing complexes of differing mobility formed by combining 1 μg of $T_{10}GT_{10}$ with increasing amounts of $A_{10}CA_{10}$. The ratios of $T_{10}GT_{10}$ to $A_{10}CA_{10}$ are: 1:0.5 (lanes 1, 2); 1:1 (lanes 3, 4); 1:1.5 (lanes 5, 6); 1:2 (lanes 7, 8); and 1:3 (lanes 9, 10). For each pair, odd and even lanes contain a trace amount of ^{32}P-labelled A or T strand, respectively. Single-stranded $A_{10}CA_{10}$ and $T_{10}GT_{10}$ are shown in lanes 11 and 12, respectively. **b.** Autoradiogram of the identical gel shown in Fig. 4a.

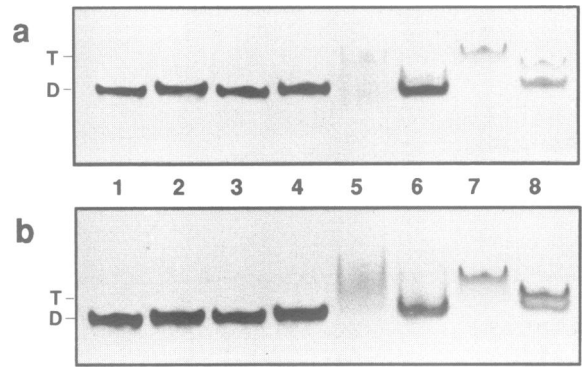

Figure 5 a. Silver stained 12% polyacrylamide gel showing complexes of differing mobility. Lanes 1 and 5 represent 1:1 and 1:2 molar ratios of $A_{10}CA_{10}$:$T_{10}GT_{10}$, respectively. Lanes 2 and 6 represent 1:1 and 1:2 molar ratios of $_pA_{10}CA_{10}$:$T_{10}GT_{10}$. Lanes 3 and 7 represent 1:1 and 1:2 molar ratios of $A_{10}CA_{10}$:$_pT_{10}GT_{10}$. Lanes 4 and 8 represent 1:1 and 1:2 molar ratios of $_pA_{10}CA_{10}$:$_pT_{10}GT_{10}$. **b.** Silver stained 12% polyacrylamide gel showing complexes of differing mobility. Lanes 1 and 5 represent 1:1 and 1:2 molar ratios of $A_{10}TA_{10}$:$T_{10}AT_{10}$, respectively. Lanes 2 and 6 represent 1:1 and 1:2 molar ratios of $_pA_{10}TA_{10}$:$T_{10}AT_{10}$. Lanes 3 and 7 represent 1:1 and 1:2 molar ratios of $A_{10}TA_{10}$:$_pT_{10}AT_{10}$. Lanes 4 and 8 represent 1:1 and 1:2 molar ratios of $_pA_{10}TA_{10}$:$_pT_{10}AT_{10}$.

triplex stability upon 5′-phosphorylation was readily discernible by silver staining, as illustrated in lanes 6 and 7 of Figs. 5a and 5b: triple helix was detected only when the T strand was phosphorylated. This experiment clearly demonstrates that even a triple helix composed of two phosphorylated T strands is more stable than a triple helix containing a single phosphorylated A strand.

Melting experiments were done to quantify the effect of phosphorylation on triplex stability. For the cases of A:TA and G:CG in the Y:XY position, melting curves were measured for all possible combinations of association of a single strand with a duplex: no phosphate on either strand, phosphate on $A_{10}XA_{10}$ only, phosphate on $T_{10}YT_{10}$ only, and both strands phosphorylated (Figs. 6a and b). For the system comprised of $A_{10}TA_{10}$ and $T_{10}AT_{10}$ strands in a 1:2 ratio, similar stabilities for triplex dissociating to duplex and single strand were observed when neither strand was phosphorylated and when the T strands were phosphorylated. However, the triple helix with a phosphorylated $A_{10}TA_{10}$ strand exhibited a T_m lower by 2°C. When all three strands comprising the triplex were phosphorylated, the T_m dropped about 8°C relative to unphosphorylated strands (see Fig. 6a and Table 1). Triple helices with $T_{10}GT_{10}$ and $A_{10}CA_{10}$ exhibited similar results with regard to phosphorylation (see Fig. 6b and Table 1). The order of stability is: no phosphate on either strand > phosphate on both $T_{10}GT_{10}$ strands > phosphate on the $A_{10}CA_{10}$ strand > phosphate on all three strands. The results of the thermodynamic melting experiments are consistent with those of the gel mobility experiments.

To provide further insight into the destabilization caused by the 5′-phosphate of association of a single strand to a duplex target, thermodynamic parameters were determined by measuring melting curves as a function of strand concentration for the triple helices of G:CG with no phosphate on either strand and with the phosphorylated A strand combined with the nonphosphorylated T strand. The $1/T_m$ vs. log (C_t/6) plots are shown in Fig. 7, and thermodynamic parameters are listed in

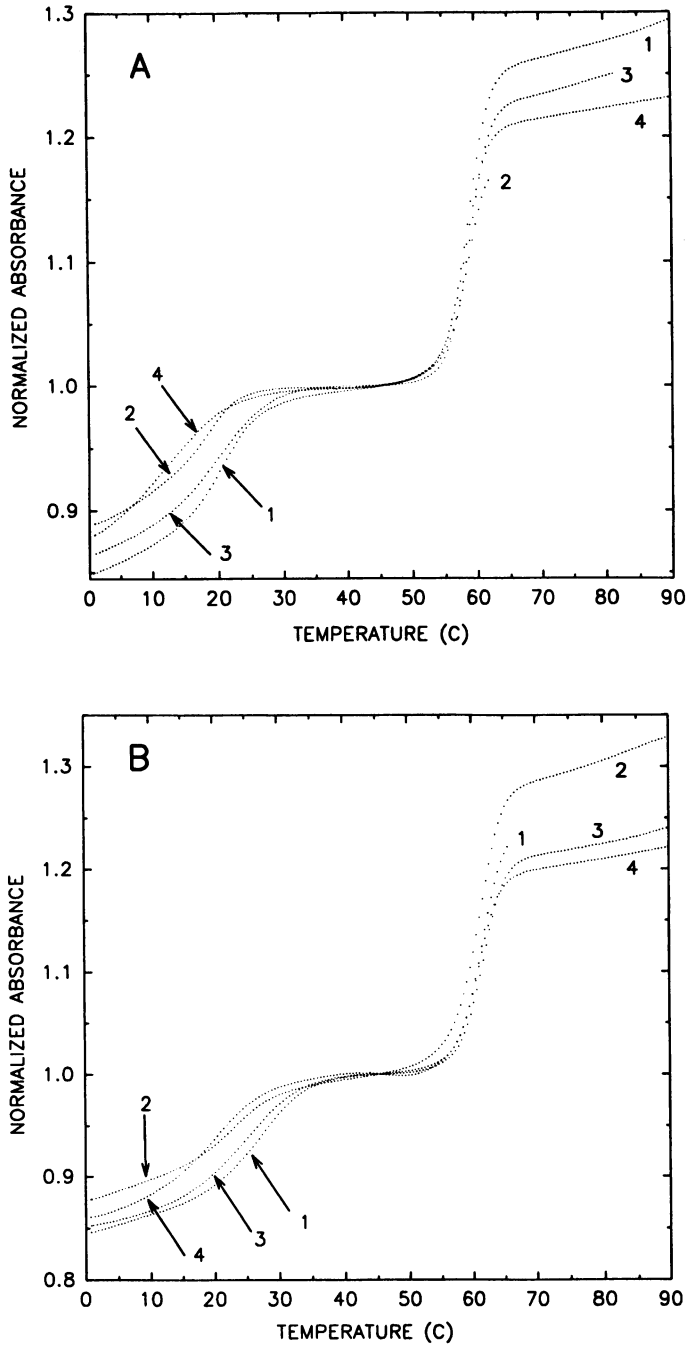

Figure 6 a. Normalized absorbance at 259 nm vs. temperature for triple helices with A:TA in the Y:XY position. Absorbances were normalized by dividing by the absorbance at 45°C. Curve 1 represents $A_{10}TA_{10}$:$T_{10}AT_{10}$ in a 1:2 ratio. Curve 2 represents $_pA_{10}TA_{10}$:$T_{10}AT_{10}$ in a 1:2 ratio. Curve 3 represents $A_{10}TA_{10}$:$_pT_{10}AT_{10}$ in a 1:2 ratio. Curve 4 represents $_pA_{10}TA_{10}$:$_pT_{10}AT_{10}$ in a 1:2 ratio. Concentrations of oligonucleotides are listed in Table I. **b.** Normalized absorbance at 259 nm vs. temperature for triple helices with G:CG in the Y:XY position. Absorbances were normalized by dividing by the absorbance at 45°C. Curve 1 represents $A_{10}CA_{10}$:$T_{10}GT_{10}$ in a 1:2 ratio. Curve 2 represents $_pA_{10}CA_{10}$:$T_{10}GT_{10}$ in a 1:2 ratio. Curve 3 represents $A_{10}CA_{10}$:$_pT_{10}GT_{10}$ in a 1:2 ratio. Curve 4 represents $_pA_{10}CA_{10}$:$_pT_{10}GT_{10}$ in a 1:2 ratio. Concentrations of oligonucleotides are listed in Table I.

Table 2. The free energy at 25°C, $\Delta G°_{25}$, for the triplex with no terminal phosphate is 1 kcal/mol more favorable than that of the triplex with a phosphorylated A strand.

Table 1. Thermodynamic parameters from single melting curves for the association of single strand DNA to duplex target[a]

Triplex	Concentration,M[b]	T_m,°C	-ΔH° (K cal/mol)	-ΔS° (eu)	$-\Delta G°_{25}$ (k cal/mol)
$T_{10}GT_{10}$ $A_{10}CA_{10}$ $T_{10}GT_{10}$	6.40 x 10^{-5}	27.2	76.5	232.1	7.30
$T_{10}GT_{10}$ $pA_{10}CA_{10}$ $T_{10}GT_{10}$	6.23 x 10^{-5}	23.1	85.4	265.5	6.24
$pT_{10}GT_{10}$ $A_{10}CA_{10}$ $T_{10}GT_{10}p$	7.47 x 10^{-5}	24.6	58.6	174.2	6.66
$pT_{10}GT_{10}$ $pA_{10}CA_{10}$ $T_{10}GT_{10}p$	6.91 x 10^{-5}	19.5	64.4	197.6	5.49
$T_{10}AT_{10}$ $A_{10}TA_{10}$ $T_{10}AT_{10}$	6.93 x 10^{-5}	20.5	89.0	280.4	5.40
$T_{10}AT_{10}$ $pA_{10}TA_{10}$ $T_{10}AT_{10}$	6.36 x 10^{-5}	18.8	94.8	302.1	4.73
$pT_{10}AT_{10}$ $A_{10}TA_{10}$ $T_{10}AT_{10}p$	7.00 x 10^{-5}	20.1	61.3	186.7	5.64
$pT_{10}AT_{10}$ $pA_{10}TA_{10}$ $T_{10}AT_{10}p$	5.66 x 10^{-5}	(12.3)			

[a] Although estimated errors in ΔG°, ΔH°, and ΔS° are ±2%, ±10%, and ±10%, respectively, additional significant figures are given to allow accurate calculation of T_m and other parameters.
[b] Concentration is the sum of the single strand + duplex target.

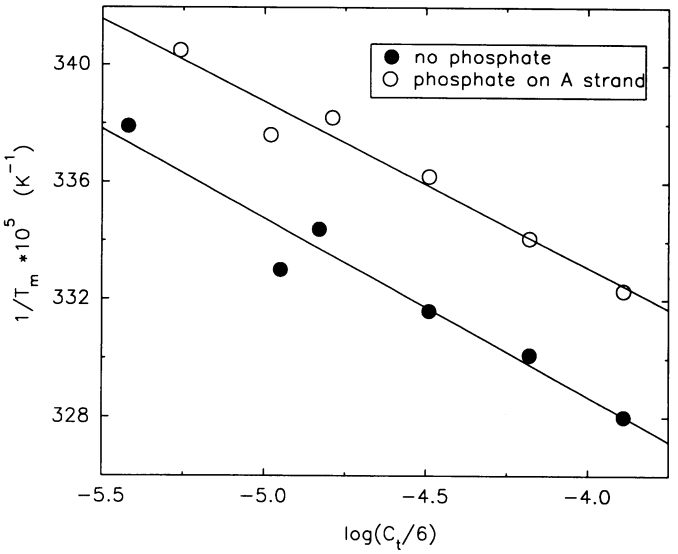

Figure 7. Plots of $1/T_m$ vs. log (C_t/6) for triplex with G:CG in the Y:XY position. Plots for triplex with no phosphorylated strands (filled circle) and triplex composed of $_pA_{10}CA_{10}$:$T_{10}GT_{10}$ in a 1:2 ratio (open circle) are depicted. C_t is the total strand concentration.

The effect of the 5′-phosphate on the stability of double-stranded DNA was compared to that of triplex. In contrast to its effect on triplex stability, the 5′-phosphate did not affect the melting temperature of duplex appreciably. Melting temperature of duplex composed of $A_{10}CA_{10}$ and $T_{10}GT_{10}$ strands was 61.1 ± 0.4°C at the concentrations listed in Table I, independent of phosphorylation of either or both strands. Melting temperature of duplex containing $A_{10}TA_{10}$ and $T_{10}AT_{10}$ strands was 58.6 ± 0.3°C at the concentrations listed in Table I, once again, independent of phosphorylation of either or both strands. Analysis of the data for $A_{10}CA_{10}$ and $pA_{10}CA_{10}$ forming duplexes with $T_{10}GT_{10}$ at different total strand concentrations also indicated that the duplex T_m was essentially independent of phosphorylation.

Table 2. Thermodynamic parameters for the association of single strand DNA to duplex target from a series of concentrations[a]

Triple Helix	1/T_m vs. log C_t/6				Curve fit parameters			
	$-\Delta G°_{25}$ (kcal/mol)	-ΔH° (kcal/mol)	-ΔS° eu	T_m,°C[b]	$-\Delta G°_{25}$ (kcal/mol)	-ΔH° (kcal/mol)	-ΔS eu	T_m,°C[b]
No phosphate								
$T_{10}GT_{10}$ $A_{10}CA_{10}$ $T_{10}GT_{10}$	6.97	75.58	230.13	27.7	6.97	77.83	237.65	27.7
Phosphate on A strand								
$T_{10}GT_{10}$ $pA_{10}CA_{10}$ $T_{10}GT_{10}$	6.02	80.02	248.21	24.0	5.98	80.22	249.00	23.9

[a] Although estimated errors in ΔG°, ΔH°, and ΔS° are ±2%, ±10%, and ±10%, respectively, additional significant figures are given to allow accurate calculation of T_m and other parameters.
[b] T_m is calculated for $C_t = 1.5 \times 10^{-4}$ M.

DISCUSSION

An effect of 5′-phosphorylation on the stability of triple helical DNA has been demonstrated by both gel electrophoresis and UV melting methods. A 5′-phosphate on the purine middle strand of a triple helix lowers the stability of triple helix formation by approximately 1 kcal/mol at 25°C. The middle strand is involved in both Watson-Crick and Hoogsteen base pairing. In contrast, a 5′-phosphate on each of the pyrimidine strands, which are involved in either Watson-Crick or Hoogsteen base pairing, has a smaller effect on the stability of triple helix (see Table 1). This same trend is observed when both pyrimidine strands are phosphorylated such that the triplex has one extra negative charge in comparison to the triplex with the phosphate on the middle strand. The destabilizing effect of the terminal phosphate on the middle strand is largely due to an unfavorable entropy change for formation of triplex rather than an enthalpy change.

The destabilizing effect of the 5′-phosphate on the middle strand of a DNA triplex contrasts with the effect of a 5′-phosphate on the stability of DNA and RNA duplexes. The 5′-phosphate did not affect appreciably the melting temperature of duplex DNA. RNA duplex stability increases about 0.2 kcal/mol in the presence of a 5′-phosphate (18). This phenomenon is thought to be due to a more rigid sugar conformation of the single-stranded RNA, caused by steric hindrance resulting from the 5′-phosphate (19,20).

The destabilizing effect of the 5′-phosphate was more pronounced for triplex involving mismatch triplets compared to those containing canonical triplets. This dependence is interesting, given that the mismatches are not close to the phosphorylation site. Structural characterization is needed to explain the destabilization effect further.

A 5′-^{32}P label is often used as a tracer for nucleic acid strands with the assumption that the ^{32}P label does not affect the

equilibria being studied. The results from this work indicate that this assumption is not valid for formation of triplexes. Evidently, the presence of a 5′-phosphate on the middle strand destabilizes the triplex. This is the reason that different results were obtained for the detection of triplex by silver staining and autoradiography.

REFERENCES

1. Arnott,S. and Bond,P.J. (1973) *Nature*, **244**, 99–101.
2. Felsenfeld,G., Davies,D.R. and Rich,A. (1957) *J. Am. Chem. Soc.*, **79**, 2023–2024.
3. Hoogsteen,K. (1959) *Acta Cryst.*, **12**, 822–823.
4. Morgan,A.R. and Wells,R.D. (1968) *J. Mol. Biol.*, **37**, 63 –80.
5. Moser,H.E. and Dervan,P.B. (1987) *Science*, **238**, 645–650.
6. Griffin,L.C. and Dervan,P.B. (1989) *Science*, **245**, 967–971.
7. Mergny,J.L., Sun,J.S., Rougee,M., Montenay-Garestier,T., Barcelo,F., Chomilier,J. and Helene, C. (1991) *Biochemistry*, **30**, 9791–9798.
8. Broitman,S.L., Im,D.D. and Fresco,J.R. (1987) *Proc. Natl. Acad. Sci. USA*, **84**, 5120–5124.
9. Beal,P.A. and Dervan,P.B. (1991) *Science*, **251**, 1360–1363.
10. Cooney,M., Czernuszewicz,G., Postel,E.H., Flint,S.J. and Hogan,M.E. (1988) *Science*, **241**, 456–459.
11. Durland,R.H., Kessler,D.J., Duvic,M., Pettitt,B.M., and Hogan,M.E. (1991) *Biochemistry*, **30**, 9246–9255.
12. Postel,E.H., Flint,S.J., Kessler,D.J., and Hogan,M.E. (1991) *Proc. Natl. Acad. Sci. USA*, **88**, 8227–8231.
13. Yoon,K., Hobbs,C.A., Koch,J., Sardaro,M., Kutny,R. and Weis,A.L. (1992) *Proc. Natl. Acad. Sci. USA*, **89**, 3840–3844.
14. Chamberlin,M.J. (1965) *Proc. Fed. Am. Soc. Exp. Biol.*, **24**, 1446–1457.
15. Riley,M., Mailing,B. and Chamberlin,M.J. (1966) *J. Mol. Biol.*, **20**, 359–389.
16. Petersheim,M. and Turner,D.H. (1983) *Biochemistry*, **22**, 256–263.
17. Borer,P.N., Dengler,B., Uhlenbeck,O.C., Tinoco,I.Jr. (1974) *J. Mol. Biol.*, **86**, 843–853.
18. Freier,S.M., Alkema,D., Sinclair,A., Neilson,T. and Turner,D.H. (1985) *Biochemistry*, **24**, 4533–4539.
19. Sundaralingam,M. (1973) *Jerusalem Symp. Quantum Chem. Biochem.*, **5**, 417–455.
20. Sundaralingam,M. (1975) In Sundaralingam,M. and Rao,S.T. (eds.), Structure and Conformation of Nucleic Acids and Protein-Nucleic Acid Interactions. University Park Press, Baltimore, MD, pp 487–524.